Nanotechnology **17** (2006) 3791–3797 doi:10.1088/0957-4484/17/15/030

Electrochemistry and electrogenerated chemiluminescence of films of silicon nanoparticles in aqueous solution

Yoonjung Bae[1], Doh C Lee[1], Elena V Rhogojina[1,2], David C Jurbergs[1,2], Brian A Korgel[1] and Allen J Bard[1]

[1] Department of Chemistry and Biochemistry, and Department of Chemical Engineering, Center for Nano- and Molecular Science and Technology, Texas Materials Institute, The University of Texas at Austin, Austin, TX 78712, USA
[2] InnovaLight Inc., 3303 Octavius Drive, Suite 104, Santa Clara, CA 95054, USA

Received 27 February 2006, in final form 2 June 2006
Published 6 July 2006
Online at stacks.iop.org/Nano/17/3791

Abstract
Films of octadecyl-capped Si nanoparticles (NPs) (diameter, 3.4 ± 0.7 nm) prepared by drop-coating on indium tin oxide (ITO) showed electrogenerated chemiluminescence (ECL) for both cathodic and anodic potential sweeps in KOH solutions containing peroxydisulfate. The redox potentials of the Si NPs can be estimated as approximately -0.9 and $+0.95$ V (versus Ag|AgCl) based on the anodic potential for the onset of ECL minus the ECL peak energy. The ECL exhibits a relatively broad spectrum (FWHM = 160 nm) with a peak wavelength of ~670 nm (1.85 eV), similar to the photoluminescence spectra. In electrochemical studies in KOH solution in the absence of peroxydisulfate, an anodic current peak appears at about -1 V (versus Ag|AgCl) following a scan to negative potentials. A similar peak has been observed during the etching of a bulk single crystal Si electrode in alkaline aqueous solution. Unpassivated surface sites of Si NPs seem to be etched at potentials negative of the anodic oxidation peak.

Supplementary data files are available from stacks.iop.org/Nano/17/3791

Electrochemical studies of semiconductor nanoparticles (NPs) have been useful in determining the band edge energies, showing the effects of single hole or single electron charging, illuminating the role of surface states, and providing information on the stability of NPs upon electron transfer [1–8]. In a previous study, monolayer protected Si NPs (capped with octanol, octene, or octanethiol) dispersed in *N*,*N*-dimethylformamide as solvent showed discrete voltammetric current peaks associated with single electron additions [2]. The electrogenerated chemiluminescence (ECL) produced by cyclic generation of reduced and oxidized forms and recombination of electrons and holes was considerably red-shifted compared to the photoluminescence (PL) with these particles and was ascribed to emission from surface states [2]. ECL of other semiconductor NPs has been studied [4, 8, 9] and in general ECL was found to be much more sensitive to surface states of NPs than the PL [9a, 9b, 9c]. The band edge positions of Si NPs dispersed in a solvent [10] or of a porous Si electrode [11] have been determined from PL quenching in the presence of redox species with standard potentials appropriate for charge transfer to the conduction or valence bands of Si. The band gap estimated in these studies was larger than the PL peak energy, which was again attributed to surface state effects.

In the study reported here, the electrochemical behaviour in alkaline aqueous solution of octadecyl-capped Si NPs synthesized by laser pyrolysis of silane gas followed by chemical etching and organic monolayer passivation was investigated. Films of these nanocrystals exhibit ECL. Electrochemistry and ECL studies reveal information about the size-confined band edge positions and the stability of the Si NPs during oxidation or chemical etching. In addition, ECL of the Si NPs allows one to recognize charge transfer processes, even when the faradaic currents are small, and provides useful information about surface state energies of the particles.

For the studies reported here, Si NPs were synthesized by laser pyrolysis of silane gas using a process similar to that described previously by Huisken *et al* [12–14] and

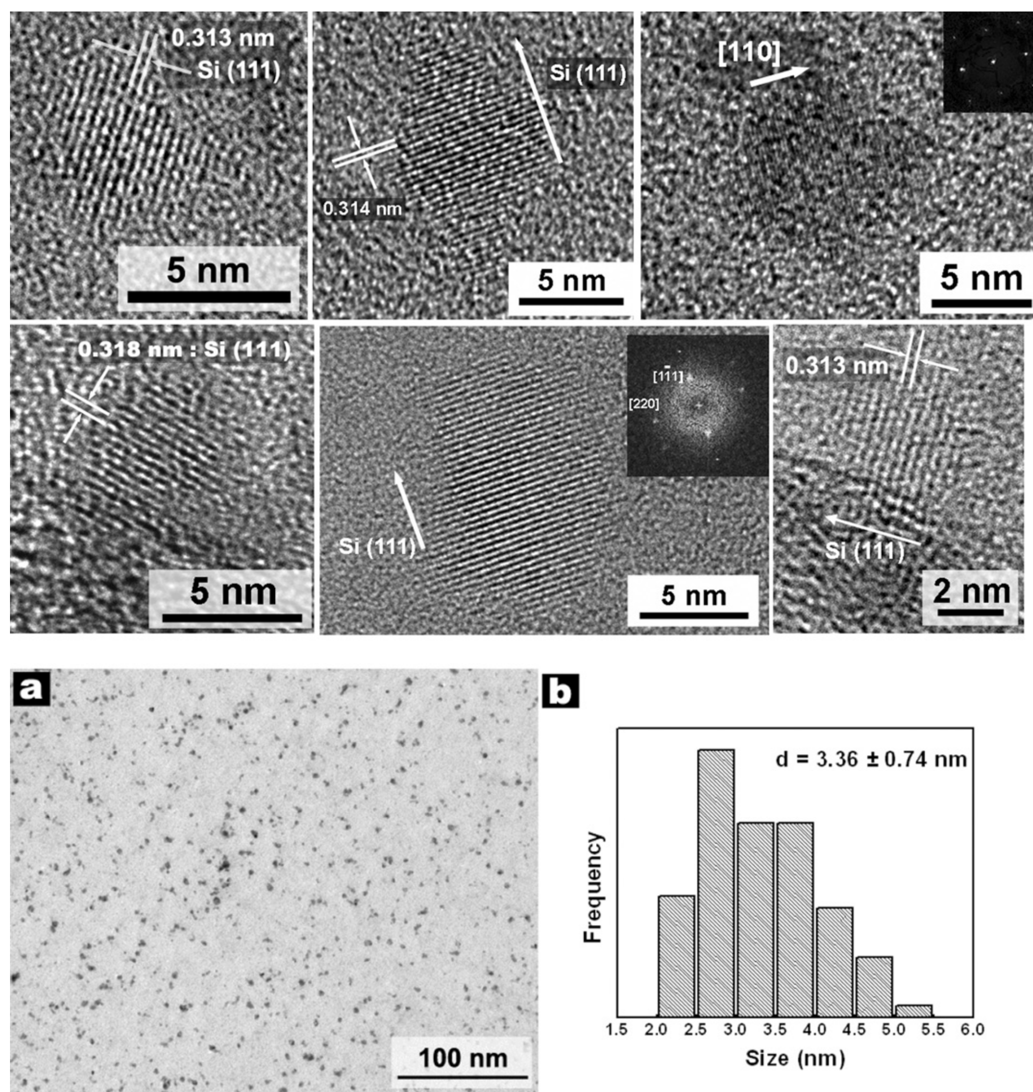

Figure 1. TEM images of octadecyl-coated Si nanocrystals. The lattice parameters measured by TEM match those expected for diamond cubic Si. The histogram was obtained from low resolution TEM images counting 400 particles, giving an average diameter d, of 3.36 nm with a standard deviation of 0.74 nm.

Li *et al* [15]. The as-made Si NPs have an average diameter of 15 nm and do not exhibit PL. To induce PL, the NPs are etched in an aqueous mixture of HF and HNO_3 to shrink the average particle diameter to ~3.5 nm to obtain NPs with bright visible luminescence. The NPs are then refluxed in 1-octadecene to chemically passivate their surfaces with an octadecyl layer [15b] that provides protection from air oxidation and chemical etching [15a, 16, 17]. The Si NPs exhibit bright visible luminescence (PL QY: 20–30%). They readily disperse in various organic solvents, such as chloroform and hexane and can be handled in air with no measurable changes in PL over many months.

Figure 1 shows TEM images of the octadecyl-coated Si NPs. The Si NPs are crystalline with diamond cubic Si crystal structure and range from 2 to 4 nm in diameter with an average diameter of 3.4 nm in the sample. Si NP films were prepared by evaporating a drop of ~0.04 ml of a dispersion of particles in 9:1 (v/v) hexane:octane on an ITO substrate (Delta Technologies Ltd, Stillwater, MN, CG-50IN-CUV) in air. ITO-covered glass slides were cleaned in a boiling 2 M KOH in 2-propanol for 20 min, followed by rinsing with distilled water and baking at 120 °C. The clean ITO surface was treated with 3-(mercaptopropyl) trimethoxysilane (MPS) to make it hydrophobic [18]. Then NP-dispersed solution was cast on the MPS-treated ITO substates. The concentration of the particles in the solution was controlled by adjusting the absorbance of the dispersion at 450 nm to ~0.45. The Si NP film (represented as ITO/MPS/Si NP) was immersed in 10 mM 1,7-heptanediamine in methanol for 10 s to link the NPs [18]. However, we found that both silane and diamine treatments did not cause a significant difference in the electrochemistry and ECL response of Si NP films compared to ones made simply by drop coating on untreated ITO. The drop-coated Si NP film was cured at 70 °C for 3–4 h. The Si NP film thickness was ~500 nm as measured by tapping mode atomic force microscopy (AFM, see figure 1S in the supporting information

available at stacks.iop.org/Nano/17/3791). Electrochemistry and ECL experiments were carried out in 0.1 M KOH with or without 0.1 M $K_2S_2O_8$, with Pt wire and Ag|AgCl as counter and reference electrodes, respectively. The solutions were not deaerated. The film area dipped into the solution was about 1.05 cm^2 (1.5 cm $\times$ 0.7 cm). Instrumental details for electrochemistry and ECL are described elsewhere [4].

ECL studies were first carried out with the film in 0.1 M KOH, with 0.1 M $K_2S_2O_8$ added as an ECL coreactant [19]. Figure 2 shows the cyclic voltammetry (CV) and ECL of (A) a blank surface-modified ITO substrate (ITO/MPS/diamine) and (B) and (C) a Si NP film (ITO/MPS/Si/diamine) with different scan directions. Peroxydisulfate can be reduced to produce a strong oxidizing agent, the sulfate radical, equation (1), which can inject a hole into a Si NP, equation (2). With the surface modified ITO substrate in the absence of Si NPs, cathodic current began to flow at -0.3 V, earlier than the blank in KOH alone, due to the reduction of peroxydisulfate on ITO. Background ECL appeared at -0.8 V with an intensity of less than 5 nA, independent of the potential scan direction. The Si NP film produced a large ECL signal when scanned to negative potentials beyond -0.95 V, which can be attributed to radiative recombination of electrons of negatively charged Si particles with holes injected by the sulfate radicals into the valence band, as described in the following series of reactions:

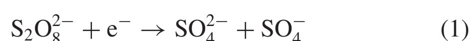

$$S_2O_8^{2-} + e^- \rightarrow SO_4^{2-} + SO_4^- \quad (1)$$

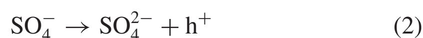

$$SO_4^- \rightarrow SO_4^{2-} + h^+ \quad (2)$$

$$Si + e^- \rightarrow Si^- \quad (3)$$

$$Si^- + h^+ \rightarrow Si + \text{light}. \quad (4)$$

A large ECL signal was also observed when scanning to positive potentials. The ECL observed at positive electrode potentials also occurred in the absence of peroxydisulfate as discussed below. Note, however, that the ECL observed at negative potentials did not occur in the absence of peroxydisulfate. While the ECL shown in figure 2 involved scanning between anodic and cathodic limits, ECL occurred on an initial scan from 0 V in either direction. The CV and ECL behaviour was observed reproducibly from the same film of Si NPs after 1 day storage in air (see the dotted lines in figure 2(B)). ECL was also measured with different Si film thicknesses in the presence of peroxydisulfate to observe the effect of film thickness on ECL intensity (see figure 2S in the supporting information available at stacks.iop.org/Nano/17/3791). The film thickness was controlled by repeated drop-coating of Si NPs. As the layer thickness increased, the PL became more intense but the current and ECL intensity decreased, probably because of hindered charge transfer through the thick film. The optimum response in ECL was found with a film thickness of ~500 nm.

The potentials for the onset of an ECL process can provide useful estimates for band edge positions, even when the voltammetric behaviour is not very well defined, since electron or hole injection is usually required for emission from the NPs. The electrode potentials at the onset of ECL in figure 2 are -0.9 and $+1.6$ V and are not dependent on the potential scan direction as shown in figures 2(B) and (C). The ECL onsets were determined by comparison with ECL curves

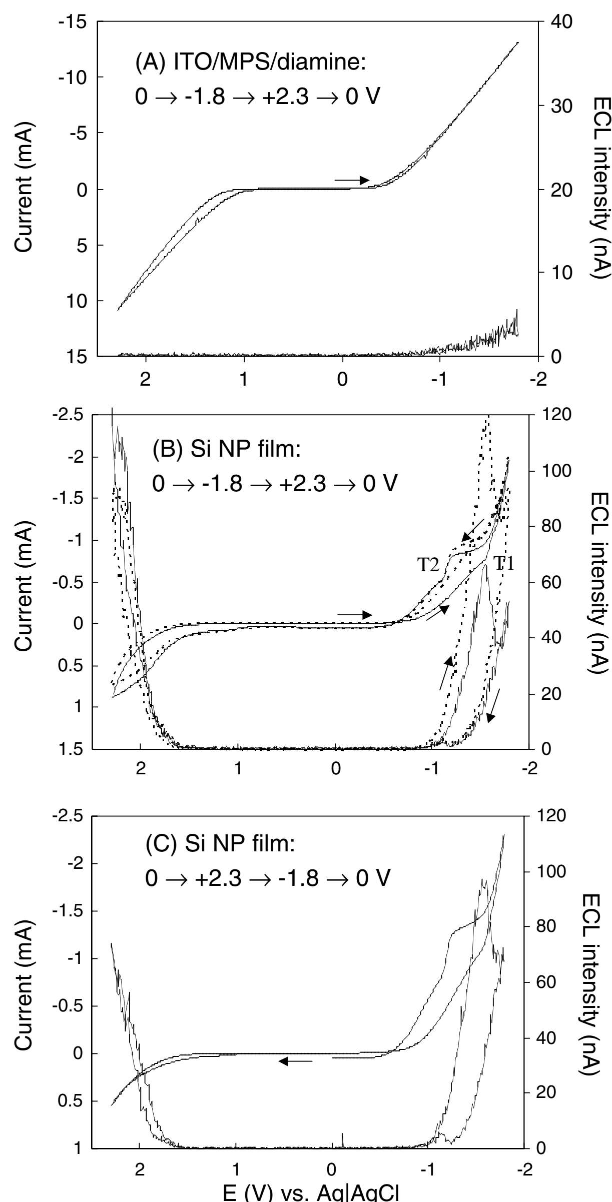

Figure 2. Cyclic voltammograms and the corresponding ECL potential curves (scan rate: 1 V s^{-1}) of (A) ITO/MPS/diamine and ((B) and (C)) ITO/MPS/Si NPs/diamine (area = 1.05 cm^2) in 0.1 M KOH + 0.1 M $K_2S_2O_8$ with different scan directions. The dotted lines were obtained from the same film of Si NPs after 1 day storage in air.

of the surface modified ITO in figure 2(A) since the blank substrate shows a weak ECL at negative potentials. Kooij *et al* [20] observed electroluminescence from a porous Si electrode immersed in a peroxydisulfate solution, where the onset of emission from the Si (~−1.1 V versus SCE) appeared at about the potential of water reduction, that is, at a potential more negative than that for the onset of peroxydisulfate reduction (−0.7 V versus SCE). Photochemical experiments led them to conclude that holes were not injected into the valence band (VB) of the Si electrode during peroxydisulfate reduction and they proposed that interaction of a peroxydisulfate or sulfate species with the Si surface could block VB hole injection until

the hydrogen evolution reaction occurs at the Si surface. This effect did not occur with the Si NP film, where the onset of ECL (−0.9 V) took place at a potential only slightly negative of that for the onset of cathodic current of peroxydisulfate reduction (−0.8 V).

Note also that in the voltammograms, the Si NP film blocks electrochemical processes on the modified ITO surface. For example, the overall current for peroxydisulfate reduction decreased about 10 times compared to the blank ITO substrate, indicating a densely packed electrically insulating Si NP film on the ITO surface. (Similar blockage and decreased currents with the Si film were also found in the absence of peroxydisulfate, as described below.) The cathodic current that starts at about −0.8 V corresponds to the reduction of peroxydisulfate at the Si NP surface. The current increases slowly with the onset of ECL, signaled by a slight inflection on the forward scan and a clearer one in the reverse scan, at about −1.0 V, probably indicating the onset of electron injection into the Si NP. The sharper inflection at −1.5 V (T1) represents the onset of water reduction on Si. Electrochemistry in the negative potential region will be discussed further in the next section.

Figure 3 shows the ECL spectrum obtained from the Si NP film by pulsing between −1.6 and +2.2 V at 10 Hz in 0.1 M KOH containing 0.1 M $K_2S_2O_8$. In the ECL transients shown in figure 3(A), the ECL intensity at −1.6 V, attributed to holes injected by sulfate radicals (generated by the reduction of coreactant) reacting with electrons, is much larger than the intensity at a positive potential step to +2.2 V. The ECL spectrum (figure 3(B), solid line) shows red emission with a peak wavelength of ∼670 nm (1.85 eV), which is similar to PL peak wavelength (figure 3(B), dotted line) of the NP film. Red PL of Si NPs (PL peak energy: 1.9 eV) [10] or of porous Si (PL peak energy: 2.0 eV) [11] has been attributed to surface state-related emission in some cases. In these studies, the band edge positions were estimated from Si PL quenching with redox species to yield band gaps of 2.3 [10] and ⩾2.60 eV [11], respectively, which were significantly larger than the PL peak energies. ECL from surface states has been observed from semiconductor NPs such as Si [2], Ge [9c], and CdSe [9a], [9b], which was substantially red-shifted from the PL. For example, the Si NPs showed an intense violet PL (∼420 nm) possibly assigned to direct electron–hole recombination. The ECL of these particles had a maximum intensity at 640 nm, and it was ascribed to a surface state emission. In the case of the octadecyl-capped Si NPs presented here, the PL and ECL peaks were positioned at nearly the same wavelength, equivalent to an energy of ∼1.85 eV. In some cases, the surface capping molecule chemistry on Si NPs has been found to modify the band gap energy [21, 22]. Warner *et al* observed that the PL intensity maxima of 1–2 nm Si NPs coated with allylamine- or 1-heptene shifted depending on the capping molecule chemistry [23].

Figure 4 shows CV and ECL responses of (A) a surface modified ITO substrate (ITO/MPS/diamine) blank and ((B) and (C)) Si NP film (ITO/MPS/Si/diamine) in KOH solution without peroxydisulfate. In the surface modified ITO substrate as shown in figure 4(A), cathodic and anodic current started to flow at about −1 and +0.7 V, respectively, and there was no ECL signal. The absence of ECL here, but not in the

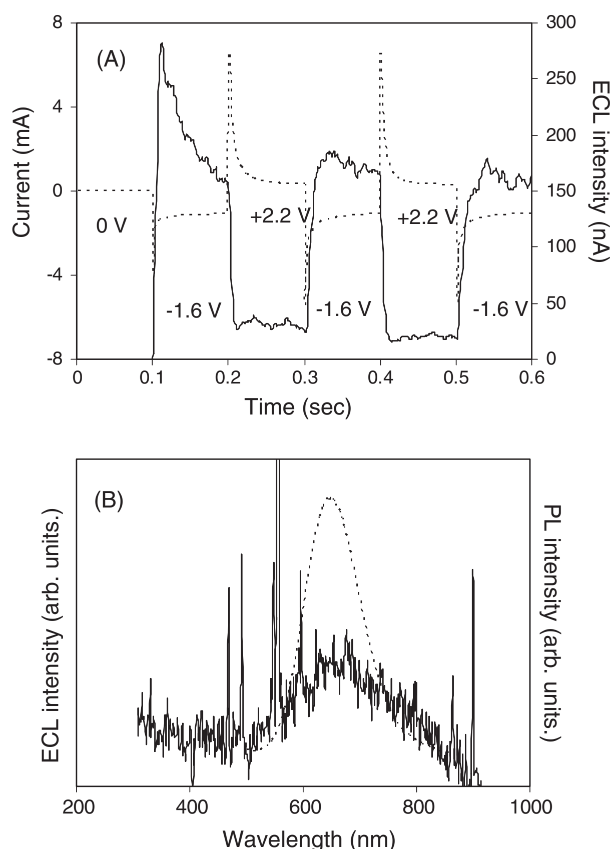

Figure 3. (A) ECL signal (solid line, right axis) and current (dashed line, left axis) as function of time and (B) ECL spectrum (integration time: 5 min) of Si NP film in 0.1 M KOH + 0.1 M $K_2S_2O_8$ obtained by stepping potentials between −1.6 and +2.2 V (versus Ag|AgCl) at 5 Hz. The dotted line is the PL spectrum (λ_{ex} = 435 nm) of Si NPs in 9:1 (v/v) hexane:octane.

presence of peroxydisulfate, indicates that it is some process involved in the reduction of that species which causes the weak emission. When the substrate with the Si NP film was scanned towards positive potentials, the current onset occurred at more positive potentials than the blank and showed an ECL signal starting at +1.7 V that increased as the potential became more positive (figure 4(B)), similar to the behaviour seen in figure 2. This suggests that the ECL at positive potentials is not connected with peroxydisulfate. With an initial scan in the negative potential direction (figure 4(C)), the current again started at more negative potentials than the blank and, unlike the behaviour with peroxydisulfate, no ECL signal was observed. Furthermore, no ECL was observed at negative potentials (in the absence of peroxydisulfate) when the potential was scanned from very positive values to the negative potential region to observe if there was an ECL by electron/hole annihilation in the Si NPs.

The Si NP film shows interesting voltammetric behaviour: a cathodic current peak (C1) at −1.53 V on the scan to negative potentials (from 0 to −1.8 V) and an anodic current peak (A1) at −1.07 V in the reverse potential scan (figure 4(C)). In cases of a bulk single crystalline or porous Si substrate, anodic oxidation and potential-dependent etching of silicon has been observed in alkaline aqueous solution, where etching was

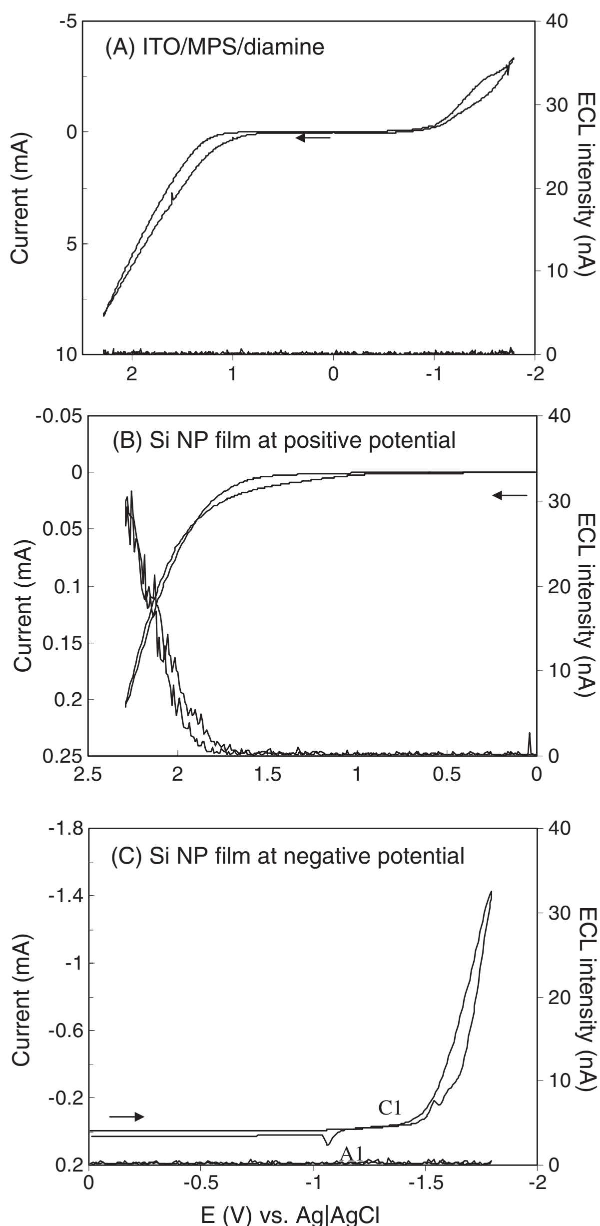

Figure 4. Cyclic voltammograms and the corresponding ECL potential curves (scan rate: 1 V s^{-1}) of (A) ITO/MPS/diamine and (B) and (C) ITO/MPS/Si NPs/diamine (area = 1.05 cm^2) in the positive and negative potential regions in 0.1 M KOH.

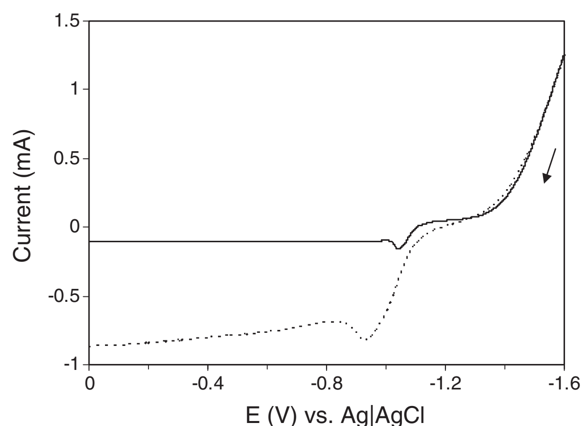

Figure 5. Voltammograms of a Si NP film in 0.1 M KOH. Potential is scanned from −1.6 to 0 V with scan rates of 0.1 V s^{-1} (solid line) and 1 V s^{-1} (dotted line).

stopped at potentials positive of an anodic current that leads to formation of an oxide layer. The observed anodic current was explained as electron injection into the bulk Si during an etching process [24–30]. Bressers *et al* [28] proposed a surface energy state consisting of an intermediate in the Si etching process, which can cause an electronless reduction of an oxidizing agent (ferricyanide) or an electron addition into the bulk Si. The diffusion-controlled reduction current of ferricyanide decreased at potentials negative of the anodic peak potential due, in part, to the electronless reduction of ferricyanide. The surface energy state of an etch-intermediate was proposed to inject electrons into bulk silicon at the peak potential of the anodic process.

The voltammetric behaviour of our Si NP film in the negative potential region in figure 4 can be explained in a similar mechanism through dissolution and oxide formation of Si NPs depending on the applied potential. In a potential scan from 0 to −1.8 V, the cathodic current peak (C1) that appears at −1.53 V and increases strongly at more negative potentials probably is related to water reduction at the Si or ITO surface. In the reverse potential scan, the Si NP film shows an anodic peak, A1, at −1.07 V which means an electron injection into the Si by an electron donor as a result of a reaction at potentials negative of the anodic peak. Figure 5 shows an increase of the anodic peak current with a positive shift of the peak potential as the scan rate increased from 0.1 to 1 V s^{-1}. The amount of charge involved in the reaction was estimated from the area under the anodic current peaks, ∼52 μC. The anodic oxidation is related to a NP surface species. A scan rate dependent anodic current was also observed at a crystalline n-type ⟨111⟩ Si substrate [26].

The peak potentials of C1 and A1 in KOH solution are similar to those of T1 and T2 labeled in figure 2 in the presence of peroxydisulfate. Two CVs, figure 2(B) in 0.1 M KOH + 0.1 M $K_2S_2O_8$ and figure 4(C) in 0.1 M KOH, are overlaid in figure 6. At potentials negative of peak T1 and C1, water reduction can occur and cause the cathodic current to increase strongly. At T2, electron injection into the conduction band of Si occurs, similar to the anodic current peak A1 in KOH. Figure 2 shows a small ECL wave at T2 in the presence of peroxydisulfate and the small ECL wave is consistent with electron injection into the conduction band and a radiative recombination of the injected electrons and valence band holes at T2. However, the current at T2 on the reverse scan represents an anodic contribution superimposed on the overall cathodic one due to reduction of peroxydisulfate. Compared to the steep current slope from T2 to 0 V, a smaller current slope from −1.5 V to T2 might be attributed in part to electronless reduction of peroxydisulfate during a silicon etching process, analogous to Bressers *et al* [28] proposed reduction of ferricyanide by an etch intermediate. With octadecyl-capped Si NPs, oxide formation or etching of Si could occur at exposed Si surface sites (H-terminated

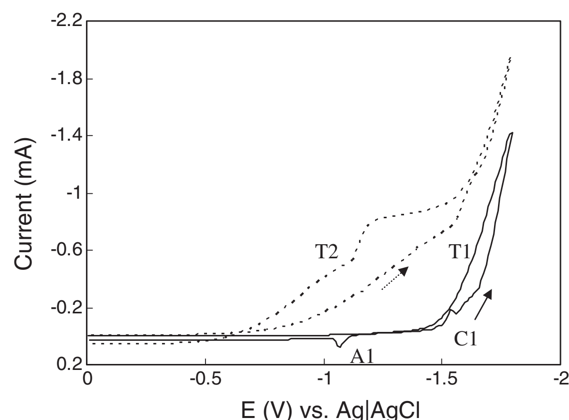

Figure 6. Comparison of cyclic voltammograms of Si NP films in KOH (solid line, the same as in figure 2(B)) and KOH $+K_2S_2O_8$ (dotted line, the same as in figure 4(C)).

Si surface) under the octadecyl layer that protects the Si NP surface from oxidation and chemical etching.

ECL during the scan to positive potentials is unexpected, because there is no obvious reductant in the 0.1 M KOH or formed at the positive potentials to donate an electron to the electrogenerated hole in the positively charged Si NP to form an excited state. The ECL is weak compared to that in the cathodic region in the presence of peroxydisulfate. It is possible that an electron donor is present in the Si sample; however, there is no obvious candidate. The components in the Si sample as synthesized and separated include octadecyl-capped Si NPs ($CH_3(CH_2)_{16}CH_2$–Si), residual 1-octadecene, and solvents used for processing, such as chloroform, IPA, and chlorobenzene. There should only be trace amounts of strongly adsorbed solvents left on the Si particles, because the film was held at 70 °C for more than 3 h before the experiment. A reducing agent might be formed by oxidation of an impurity acting as a coreactant to form a reductant by bond cleavage (as found in ECL with oxalate or tri-n-propylamine), but a candidate for such an adventitious coreactant is not clear. The ECL onset at positive potential may correspond to the oxidation of the adventitious coreactant, whereas the oxidation of NPs can occur at potentials less positive than that of the coreactant species. This could be a reason for the wide onset separation of ECL (figure 2).

In summary, CV of octadecyl-capped Si NP films shows reduction of water and peroxydisulfate in KOH and an anodic oxidation peak around −1 V (versus Ag|AgCl) following a cathodic sweep. The anodic peak has also been observed with a bulk crystalline or porous Si electrode and was explained as electron injection into the conduction band during the Si etching process. A small ECL wave at the same potential as the anodic current peak can be explained as a radiative recombination of conduction band electrons injected during the anodic oxidation and valence band holes. ECL at a negative potential in the presence of peroxydisulfate is attributed to hole injection from sulfate radicals to the valence band of a negatively charged Si NP, while the reactions leading to ECL at positive potentials is less clear. The onsets of ECL correspond to −0.9 and +1.6 V (versus Ag|AgCl). However, the ECL emission peak energy, 1.85 eV, is smaller than the band gap estimated from the potentials for the onset of ECL of about 2.5 eV. The luminescence band gap of 1.85 eV suggests an oxidation potential of the Si NPs as +0.95 V (versus Ag|AgCl). The redox potentials seem to imply both possibilities of the charge transfer reactions occurring in the band edges or surface energy states of the particles.

Acknowledgments

We thank Young Jong Lee for assistance in measuring film thickness by tapping mode AFM. The support of the National Science Foundation, Robert A Welch Foundation and Strategic Partnership for Research in Nanotechnology (SPRING) AFOSR (Air Force Office of Sponsored Research) is gratefully appreciated.

Supporting information available. AFM line profile to determine Si NP film thickness and CVs and the corresponding ECL potential curves with different film thicknesses can be found in the supporting information.

References

[1] Haram S K, Quinn B M and Bard A J 2001 *J. Am. Chem. Soc.* **123** 8860
[2] Ding Z, Quinn B M, Haram S K, Pell L E, Korgel B A and Bard A J 2002 *Science* **296** 1293
[3] Kucur E, Riegler J, Urban G A and Nann T 2003 *J. Chem. Phys.* **119** 2333
[4] Bae Y, Myung N and Bard A J 2004 *Nano Lett.* **4** 1153
[5] Poznyak S K, Osipovich N P, Shavel A, Talapin D V, Gao M, Eychmuller A and Gaponik N 2005 *J. Phys. Chem.* B **109** 1094
[6] Querner C, Reiss P, Sadki S, Zagorska M and Pron A 2005 *Phys. Chem. Chem. Phys.* **7** 3204
[7] Kucur E, Bücking W, Giernoth R and Nann T 2005 *J. Phys. Chem.* B **109** 20355
[8] Bard A J, Ding Z and Myung N 2005 *Struct. Bond.* **118** 1–57
[9a] Myung N, Ding Z and Bard A J 2002 *Nano Lett.* **2** 1315
[9b] Myung N, Bae Y and Bard A J 2003 *Nano Lett.* **3** 1053
[9c] Myung N, Lu X, Johnston K P and Bard A J 2004 *Nano Lett.* **4** 183
[9d] Poznyak S K, Talapin D V, Shevchenko E V and Weller H 2004 *Nano Lett.* **4** 693
[9e] Zou G and Ju H 2004 *Anal. Chem.* **76** 6871
[10] Germanenko I N, Li S and El-Shall M S 2001 *J. Phys. Chem.* B **105** 59
[11] Rehm J M, McLendon G L and Fauchet P M 1996 *J. Am. Chem. Soc.* **118** 4490
[12] Huisken F, Ledoux G, Guillois O and Reynaud C 2003 *Silicon Chemistry* ed P Jutzi and U Schubert (New York: Wiley-VCH GmbH & Co. KGaA)
[13] Huisken F, Hofmeister H, Kohn B, Laguna M A and Paillard V 2000 *Appl. Surf. Sci.* **154/155** 305
[14] Ehbrecht M, Ferkel H, Smirnov V V, Stelmakh O M, Zhang W and Huisken F 1995 *Rev. Sci. Instrum.* **66** 3833
[15a] Li X, He Y, Talukdar S S and Swihart M T 2003 *Langmuir* **19** 8490
Li X, He Y and Swihart M T 2004 *Langmuir* **20** 4720
[15b] Linford M R, Fenter P, Eisenberger P M and Chidsey C E D 1995 *J. Am. Chem. Soc.* **117** 3145
[16] Hua F J, Erogbogdo F, Swihart M T and Ruckenstein E 2006 *Langmuir* **22** 4363–70
[17] Hua F J, Swihart M T and Ruckenstein E 2005 *Langmuir* **21** 6054–62
[18] Guyot-Sionnest P and Wang C 2003 *J. Phys. Chem.* B **107** 7355

[19] Miao W and Choi J-P 2004 *Electrogenerated Chemiluminescence* ed A J Bard (New York: Dekker) p 223
[20] Kooij E S, Noordhoek S M and Kelly J J 1996 *J. Phys. Chem.* **100** 10754
[21] Zhou Z, Brus L and Friesner R 2003 *Nano Lett.* **3** 163
[22] Reboredo F A and Galli G 2005 *J. Phys. Chem.* B **109** 1072
[23] Warner J H, Rubinsztein-Dunlop H and Tilley R D 2005 *J. Phys. Chem.* B **109** 19064
[24] Palik E D, Faust J W, Gray H F and Greene R F 1982 *J. Electrochem. Soc.* **129** 2051
[25] Glembocki O J, Stahlbush R E and Tomkiewicz M 1985 *J. Electrochem. Soc.* **132** 145
[26] Smith R L, Kloeck B, De Rooij N and Collins S D 1987 *J. Electroanal. Chem.* **238** 103
[27] Allongue P, Kieling V and Gerischer H 1993 *J. Electrochem. Soc.* **140** 1018
[28] Bressers P M M C, Pagano S A S P and Kelly J J 1995 *J. Electroanal. Chem.* **391** 159
[29] Cattarin S, Peter L M and Riley D J 1997 *J. Phys. Chem.* B **101** 4071
[30] Cattarin S and Musiani M M 1999 *J. Phys. Chem.* B **103** 3162